ELSEVIER

Catalysis Today 64 (2001) 239–252

CATALYSIS TODAY

www.elsevier.com/locate/cattod

Simulation and interpretation of catalytic combustion experimental data

P. Canu*

Universitá di Padova, Istituto di Impianti Chimici, Via Marzolo 9, 35131 Padua, Italy

Abstract

The catalytic combustion of CH_4/air in monoliths has been simulated through a commercial numerical fluid dynamic code. The program has been suitably modified in order to describe the heterogeneous reaction at the channel walls. Different flow arrangements have been studied in an attempt to closely match an experimental investigation reported in the literature. Single step overall rate equation has been used and identification of suitable kinetic constants performed through the use of optimization techniques. A framework for kinetic investigation accounting for complex flow structure and interaction with the chemistry is suggested. The relevant and sometimes overwhelming role of transport phenomena is discussed. © 2001 Elsevier Science B.V. All rights reserved.

Keywords: Catalytic combustion; Methane; Monoliths; Reaction engineering; Modeling; Parameter fitting

1. Introduction

The relevance of catalysis in combustion for the reduction of emissions and more efficient use of fuels is largely known. A simple search on this and related journals can easily give an idea of a widespread effort to clarify the mechanisms involved, aiming at catalyst and process optimization. A general reference is the review [1]. More recently, specific issues have been addressed in the literature. Among the many aspects of catalytic combustion, mathematical modeling concentrates a large number of contributions since the 1970's [2]. The mathematical simulation is considered a valid tool for the interpretation of the mechanism and the optimization of the process. A recent review of the approaches attempted in the past and the questions still open is given by Kolackowski [3] that integrates the previous one of Pfefferle [4]. Almost all the relevant features have been addressed individually from the issue of simplifying the whole process to a monodimensional model [5] to the simulation of transient regimes [6–9] and the study of multiple steady states [10]. An active area involves the development of detailed mechanisms for the surface chemistry, correctly attempting to provide a more realistic description of the actual behavior of species at the surface and their interaction with those in the gas phase. Interestingly, efforts to properly describe the surface species tends to provide a rather simplified description of the catalytic surface morphology [11,12] just in terms of density of active sites. The issue of catalyst porosity that can influence significantly the actual rate of combustion has been pointed out experimentally [13] and theoretically [14], but apparently never discussed in conjunction with detailed surface chemistry. Detailed surface mechanisms are naturally coupled to a detailed description of the homogeneous reaction [12] whose kinetics is better known.

---

* Tel.: +39-049-8275-463; fax: +39-049-8275-461.
E-mail address: pcanu@ux1.unipd.it (P. Canu).

PII: S0920-5861(00)00528-9

Nomenclature

A	preexponential factor, cross section of the channel (m^2)
C	mass concentration (g/cm^3)
$\mathcal{D}$	diffusion coefficient (m^2/s)
E_a	activation energy (kJ/mol)
H	total enthalpy per unit mass (J/kg)
k	Arrhenius rate constant
$\dot{m}$	mass flow rate (kg/s)
N_r	number of surface reactions
P	pressure (Pa)
R_j^S	rate of surface reaction j ($kg/(m^2\,s)$)
S	source term in balance equations
T	temperature (K)
$\mathbf{U}$	velocity vector of components U, V, and W (m/s)
w_i	mass fraction of species i (kg/kg)
x_i	mole fraction of species i (kg/kg)
z	axial coordinate of the channel (m)

Greek symbols

δ	versor
ζ	bulk viscosity (Pa s)
λ	thermal conductivity (W/(m K))
μ	molecular viscosity (Pa s)
$\hat{\nu}$	mass stoichiometric coefficient of species i in reaction j (kg/kg)
ξ	methane conversion
ρ	density (kg/m^3)
ϕ	fuel equivalence ratio $(kg_{CH_4}/kg_{O_2})/(kg_{CH_4}/kg_{O_2})_{stech}$

Superscripts, subscripts, and accents

ad	adiabatic
i	species
j	reaction
k	axial measurement position (1, 2, 3, 4)
m	mixture
S	surface
T	transpose (of a vector)
0	inlet
–	average on the cross section

On the other hand, most of the theoretical studies adopt a simplified description of the chemical kinetic in terms of a single overall surface reaction, expressed through a power law equation. Obviously, the resulting parameters are extremely specific for the type of catalyst and support used. The single heterogeneous reaction models seldom add a single reaction for the gas phase oxidation [10]. Sometimes the reaction is split into a partial oxidation of CH_4 to CO and the total oxidation of the latter. This is an attempt to describe the experimental observation of significant amount of CO in the emissions following uncomplete fuel combustion. As clearly discussed in [3] and known since earlier studies [1], the interplay between chemical and physical processes does not allow oversimplifications on both sides, although a proper compromise is still a matter of discussion. In this work, we investigate the many aspects connected to a proper description of the physical process, both in terms of transport coefficients and actual geometry.

2. Description of the model

Several authors developed specific codes for the solution of the equations that describe the process of reaction and flow. Models have been proposed that describe the catalytic combustion tests in monoliths with zero dimensions [15], 1D [5], 2D [14,16], and even 3D [17], although rather infrequently. Most of the models simulate the steady-state operation of the catalyst, but a significant number of contributions dealt with transient experiments and modeling [6–9]. As pointed out by Kolackowski [3], development of detailed programs is quite an effort, and proper validation and testing requires a large amount of time. I would add that the calculation of the flow field, even for isothermal conditions, requires the application of suitable techniques described in a large body of specialized literature [18], usually unfamiliar to the catalysis community. The solution of the flow equations that neglects the hazard of unsuitable techniques can result in severe falsification of the actual behavior of the flow. The issue of ‘false diffusion’ introduced by certain discretization schemes is indeed rather well known [21]. On the other hand, people properly trained in fluid mechanics and particularly numerical solution of the flow equations (CFD, computational fluid dynamics) quite often disregard the issue of multicomponent, reactive flow. In this context, an effort should be done to merge the two field of expertise. An opportunity is given by the application of commercial fluid mechanics codes to provide a proper solution of the flow, suitably modified to introduce the actual chemistry. There are a number of commercial codes, some of them are rather widespread. That usually implies a larger number of opportunities of validation and correction of coding errors. Moreover, the availability of standard programs can help to compare simulations on a common basis, as successfully experienced with Chemkin and Surface Chemkin [11]. An interesting review of the possibilities provided by CFD to chemical reaction engineering appeared recently [18]. The commercial code used in this study is CFX [19] of AEA Technology. General assumptions made here for the simulation of a monolith channel are:

- steady-state;
- laminar flow;
- adiabatic channels;
- non-conducting walls;
- neglect of heat flux by radiation;
- neglect of thermal diffusion;
- negligible buoyancy.

Note that no assumption is made about the structure of the flow. At the monolith entrance there is a region of developing flow. The length required to develop a steady velocity profile is rather long indeed, even for isothermal flow. A reacting flow with significant temperature (i.e. density and then velocity) variations requires even longer paths to develop. Thus, the boundary conditions applied to the entrance of the channel are simply uniform velocity, without any assumption of well developed, Poiseuille-type velocity profile for $U(r)$.

According to the assumptions above, the equation solved for by the program in the specific application of interest here are summarized below.

1. Continuity equation:

$$\nabla(\rho \mathbf{U}) = 0 \tag{1}$$

2. Momentum balance:

$$\nabla(\rho \mathbf{U} \otimes \mathbf{U}) = \nabla\sigma \tag{2}$$

where the stress tensor for Newtonian fluids is given by [20]

$$\sigma = P\delta + (\zeta - \tfrac{2}{3}\mu)\nabla\mathbf{U}\delta + \mu[\nabla\mathbf{U} + (\nabla\mathbf{U})^{\mathrm{T}}] \tag{3}$$

3. Energy balance equation:

$$\nabla(\rho \mathbf{U} H) = \nabla(\lambda\nabla T) \tag{4}$$

where H is the total enthalpy, obtained by addition of the kinetic energy of the fluid to the thermodynamic contribution, h:

$$H = h(T, P) + \tfrac{1}{2}\mathbf{U} \tag{5}$$

although the kinetic term is minor at velocity typical of monolith channels.

4. Species mass balance:

$$\nabla(\rho \mathbf{U} w_i) = \nabla(\rho \mathcal{D}_{i\mathrm{m}} \nabla w_i) \tag{6}$$

where $i = \mathrm{CH_4}, \mathrm{O_2}, \mathrm{CO_2}, \mathrm{H_2O}$. The carrier is N_2. This is an approximation for multicomponent transport, where the diffusion due to other species gradients is included in the effective diffusivity coefficient $\mathcal{D}_{i\mathrm{m}}$, [20], which is a function of local composition. A species mass balance is required for any species involved in the kinetic equations. Accordingly, for a single irreversible superficial reaction between CH_4 and O_2, the CO_2 and H_2O balances can be omitted, unless their contribution to the mixture properties (μ, λ, C_p) is relevant. We chose to keep them since the computation burden is marginally affected.

In the balance equations above, density is allowed to vary with T and P according to the ideal gas equation of state. Pressure is a variable as well, so that simulations predict the pressure loss in the catalyst as well. This could be used as an additional variable to be compared to experimental measurements. Buoyancy can be easily introduced as an additional body force in the momentum equation, but neglected in the present application, because of the small vertical extent of the channels. The numerical approach implemented by CFX is based on the work of Patankar [21] with major updates and extensions [19]. The program requires to be suitably modified to simulate a heterogeneous reaction, taking place at the boundary of the domain. Moreover, the actual configuration of the experimental setup should be reproduced as closely as possible. The reaction can be introduced as a boundary condition, which is the preferred solution in the published models. We followed a different strategy, because it provides more flexibility in the analytical form of the rate expression [22]. The reaction appears as a source (or sink) of material and energy at each boundary cell, and specifically at its surface in contact with the catalyst wall. Accordingly, the ith species and the energy balance equations at the wall are modified as follows:

$$\nabla(\rho \mathbf{U} H) = \nabla(\lambda \nabla T) + S_H(T, \mathbf{w}) \tag{7}$$

$$\nabla(\rho \mathbf{U} w_i) = \nabla(\rho \mathcal{D}_{i\mathrm{m}} \nabla w_i) + S_i(T, \mathbf{w}) \tag{8}$$

Source terms are, respectively,

$$S_H(T, \mathbf{w}) = \sum_j^{Nr} (-\Delta H_j) R_j^{\mathrm{S}} \tag{9}$$

$$S_i(T, \mathbf{w}) = \sum_j^{Nr} \hat{\nu}_{ij} R_j^{\mathrm{S}} \tag{10}$$

Sources have been linearized with respect to the relevant variable (T for S_H, and w_i for S_i) only in the case of CH_4 and O_2 where a negative coefficient for the variable is guaranteed [21]. Significant improvements of convergence are obtained after linearization. Frequently, the onset of a sharp temperature and composition change along the channel, corresponding to the ignition point, makes the numerical convergence rather difficult to achieve. Suitable variation of the underrelaxation factors [19] during the iterative solution of the balance equations have been implemented, to keep the numerical solution progress smoothly.

Transport properties strongly influence the result of the simulation. The extreme activity of Pt catalysts results in a conversion rate that rapidly overtake the rate of mass transfer from and to the bulk of the fluid. In a laminar flow, the molecular diffusion coefficient is the key to the actual rate of conversion once in the mass transfer limited regime. Values have been estimated as a function of temperature, pressure and composition through the Transport Library of Chemkin [23]. Since a large amount of the flowing gas is N_2, the composition dependency can be neglected and values of the binary diffusion coefficients $\mathcal{D}_{i,\mathrm{N}_2}(T, P)$ can be used. Diffusion coefficients have been obtained through the properties estimation program [23] and then the temperature dependency at 1 bar reduced to a simple polynomial. A detailed discussion of their role is given below with reference to a specific application.

Other transport properties are less temperature-dependent. Molecular viscosity of N_2 varies between 2.9×10^{-5} and 5.4×10^{-5} Pa s between 850 and 1500 K. The temperature dependence included in the program is taken from DIPPR as

$$\mu(T) = 0.7632 \times 10^{-6} T^{0.58823} \frac{1}{1 + 67.75/T} \ (\mathrm{Pa\,s})$$

Thermal conductivity of N_2 varies between 4.5×10^{-2} and 9.4×10^{-2} J/(m K s) in the same temperature range; we used the interpolation given in [24]:

$$\lambda(T) = 3.919 \times 10^{-4} + 9.816 \times 10^{-5} T - 5.067 \times 10^{-8} T^2 + 1.504 \times 10^{-11} T^3 \ (\mathrm{W/(m\,K)})$$

Values match those obtainable by the correlation reported in [25]. Viscosity calculated from the equation reported in [9] is one order of magnitude greater than these results, possibly because of a misprint. Specific heat of the involved species was assumed temperature-dependent according to standard equations for the ideal gas state [24].

The heterogeneous reaction has been modeled as a single step. Although many recent contributions to this field help to shape a detailed surface mechanism, many aspects remain unsolved. The role of surface macrostructure and the values of the estimated kinetic parameters are still unsettled. A single step has been used many times in the past and several rate equations are available. Most of the models dealing with Pt/Al_2O_3 catalysts refer to the equation

$$R = k(T) C_{\mathrm{CH}_4} C_{\mathrm{O}_2}^{1/2} \tag{11}$$

$$k(T) = A \exp\left(\frac{-E_{\mathrm{a}}}{RT}\right) \tag{12}$$

quoted as developed by Trimm and Lam [13]. Curiously, the original work studied fiber catalysts and reports a number of kinetic equations, clearly distinguishing between porous and non-porous substrates and different temperature ranges. The expression above is not in the list, except as part of more complex Langmuir–Hishelwood type equations. Neglecting any adsorption term (i.e. low surface coverage) one gets closer to the equation above, although the consumption rate of methane, according to Trimm and Lam [13, Eq. 4], still depends upon two contributions, where the partial reaction order of O_2 is 1 and $\frac{1}{2}$. The above equation is frequently cited and used in the literature [26] with $A = 1.3 \times 10^{11}\ \mathrm{cm}^{5/2}\,\mathrm{s}^{-1}\,\mathrm{g}^{-1/2}$,

$E_a = 134.7\,\mathrm{kJ/mol}$ and C_i mass concentration ($\mathrm{g/cm^3}$), resulting in a rate of methane consumption expressed as $\mathrm{g_{CH_4}/(cm^2\,s)}$. In this work, we followed this interpretation, evaluating also the effect of different values for A and E_a. Note that the composition in Eq. (11) was expressed in [10] as molar fraction, with the same preexponential factor, apparently resulting in some inconsistency with the expression used in [26], as already observed [28]. The original study [13] also expressed all the results in terms of molar percentages (again, a 10^3 factor with respect to molar fractions) which is quite unusual in a kinetic equation, since the effect of pressure is somehow lost. Summarizing, the interpretations of Eq. (11) in terms of partial reaction orders, concentration variables, values and units of kinetic parameters given by many authors using it are not always comparable.

The kinetic equations obtained by Trimm are similar to previous investigations [6,27]. All these equations are attempts to describe the complexity of the behavior with respect to surface properties, temperature and equivalence ratio through Langmuir–Hishelwood type kinetic models. That was supposed to be the most detailed model one could achieve before the concept of microkinetics [29] evolved, resulting in the actual research on detailed surface mechanisms [12].

Summarizing, the use of a single overall reaction is a choice that can be used to simulate experimental results in very specific conditions. There is no theoretical justification in using the same equation for different experimental systems. All the equations must be considered empirical expression to account for a variety of aspects, including surface properties and temperature-dependent mechanisms. All the above justify the use of a single kinetic equation as an adaptive part [30] inside a more detailed model of the whole process, provided the transport mechanism is dominant. More details for the simulation of a specific case are given later.

3. Description of the experimental data

So far our analysis concentrated on a single set of experimental data taken from the literature [31], because of the completeness of the information provided. Shortly, natural gas is oxidized in a flow reactor containing a commercial monolith (200 cells per square inch, with square channels and 3×10^{-4} m wall thickness) with 2% Pt. The monolith is segmented into four cylindrical wafers of 0.05 m diameter and 0.02 m length, leaving 0.038 m empty space in between for measurements of intermediate temperature and conversion. Results relevant for the simulation are summarized in Table 1 as given by the authors and deduced from the figures and other data in [31]. It is worth noting that preheating of the mixture is achieved by homogeneous combustion of H_2. Such a reaction modifies the composition of the mixture fed to the monolith because it produces steam and varies the oxygen content, so that the equivalence ratio must be reevaluated accordingly. The resulting composition as calculated from the data given in the paper is reported in Table 1 in terms of mass fraction. The adiabatic temperature rise, according to the equivalence ratio is reported in Table 1 as given by the Bond et al. [31]. Values have been recalculated through the STANJAN-III code [32] and the composition reported in Table 1, obtaining slightly different results. The fuel conversion has been determined by Bond et al. [31] based on either O_2 consumption or CO_2 production without significant differences. That implies a complete conversion of methane

Table 1
Summary of experimental data[a]

Inlet conditions			
ϕ	0.18	0.3	0.39
w_{CH_4}	0.00776	0.0129	0.0167
w_{O_2}	0.172	0.171	0.171
w_{H_2O}	0.0646	0.0643	0.0639
U(m/s)	7.2	7.3	7.3
Temperature (K)			
0	846	852	850
1	850	880	900
2	860	912	1130
3	870	950	1200
4	885	1030	1280
T_{ad} [31]	1174	1364	1498
T_{ad} [32]	1155	1350	1483
CH_4 conversion (%)			
0	0	0	0
1	4	6	10
2	6	10	40
3	9	22	55
4	13.5	38	63

[a] 0, 1, 2, 3, 4 represent the axial positions, where 0 is the monolith inlet, 1, 2, 3 the gaps between wafers and 4 the outlet conditions. CO_2 is always absent in the feed.

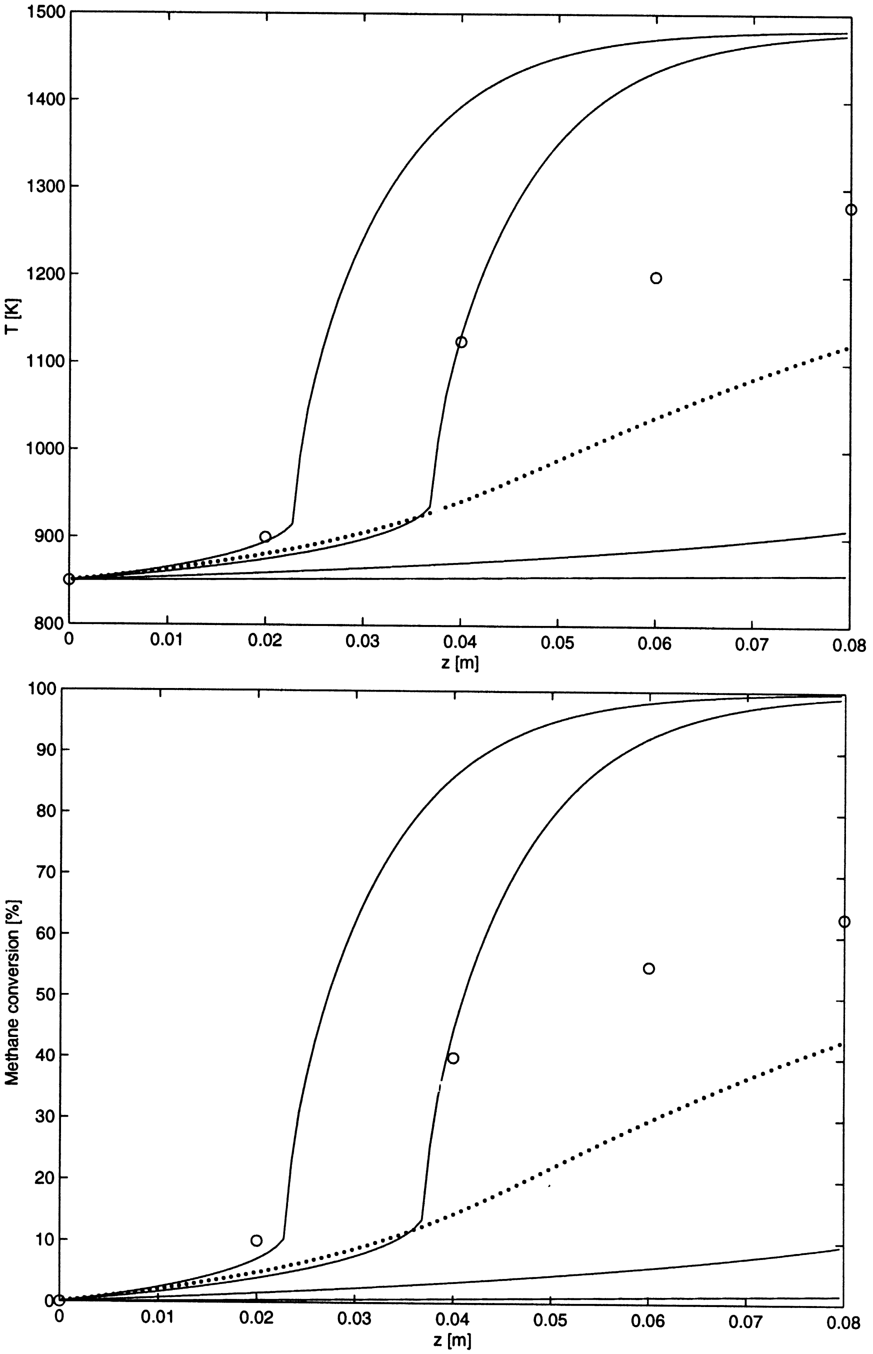

Fig. 1. Temperature and conversion profiles from a continuous channel model: (solid lines) $E_a = 134.7$ kJ/mol, $A = 1.3 \times 10^9$, 5.0×10^9, 1.0×10^{10}, 1.3×10^{10} cm$^{5/2}$ s^{-1} g$^{-1/2}$; (dotted line) $E_a = 134.7$ kJ/mol, $A = 1.3 \times 10^{11}$ cm$^{5/2}$ s^{-1} g$^{-1/2}$, diffusion coefficients divided by 10. Data from [31] at $\phi = 0.39$.

to CO_2 and H_2O without byproducts. CO has been found in very small concentration, indeed. Accordingly, the temperature rise with conversion should be linear:

$$T(z) = T_0 + \xi(T_{ad} - T_0) \tag{13}$$

where T_0 is the inlet temperature and ξ the methane conversion. Lower values would imply a conversion of methane to some partially oxidized species. Higher values are not possible. T_{ad} calculated for the production of CO_2 and H_2O is the maximum temperature rise because of the lowest value of Gibbs free energy of formation of these products among the possible ones. Apparently, some of the measured temperatures lie above values consistent with conversion. Although differences can be small, possibly due to uncertainties in reading data from the figures, this simple check can help to properly understand the experimental results, pointing out the consistency of the conversion or temperature measurements.

4. Simulation of the experimental data

The experiments described above are simulated assuming first that the intermediate temperature and conversion measurements represent values from a single continuous monolith, 0.08 m long. The approach was adopted also in the original work [31] and is quite common, although questionable, as discussed below. The square channel is modeled as a circular one to take advantage of axisymmetry and reduce to a 2D description. The equivalence criterion is the conservation of the total catalytic surface. The existence of radial gradients of relevant variables implies that

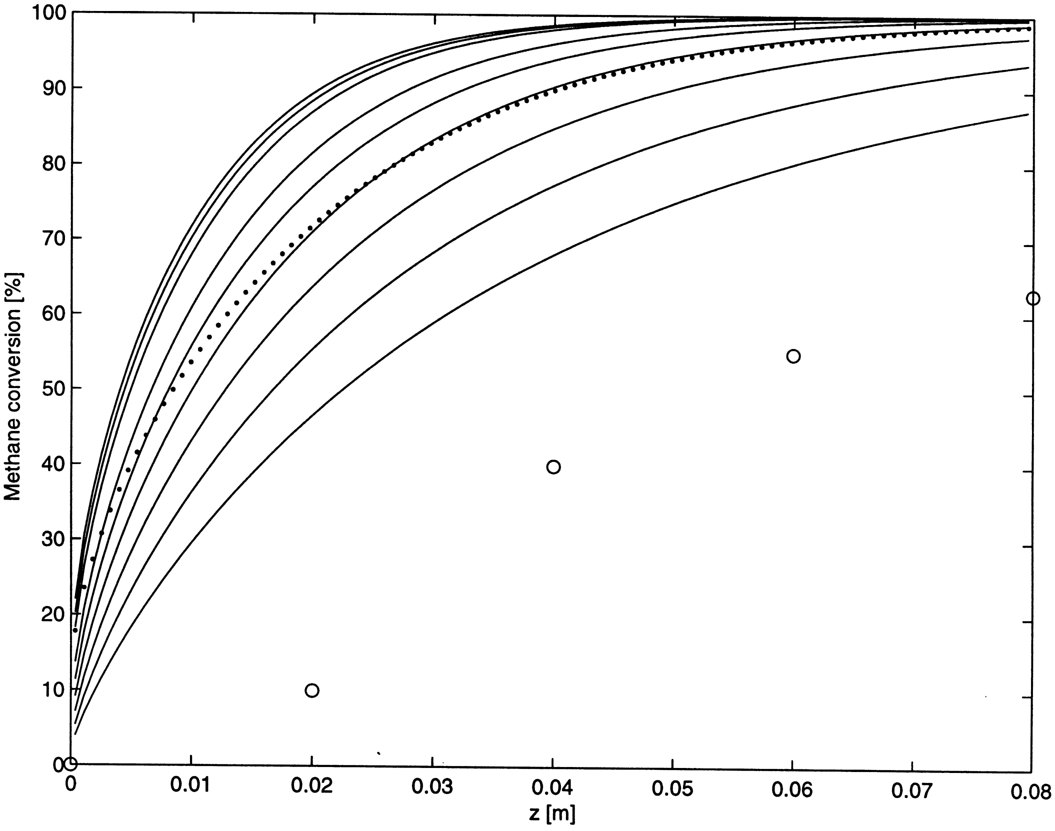

Fig. 2. Conversion profile from a continuous channel model: (solid lines) increasing k ($\log_{10} k = 3.5{:}0.5{:}5.3$); (dotted line) $\log_{10} k = 5.3$, $\mathcal{D}_{i,N_2}(T)$ halved. Data from [31] at $\phi = 0.39$.

some kind of average has to be computed in order to compare the simulation with the measurements, given at discrete axial positions. Accordingly, at any sampling point z_k, the average mass fraction of CH_4 is given by

$$\bar{w}_{CH_4}(z_k) = \frac{\int_A \dot{m} w_{CH_4}}{\int_A \dot{m}} \tag{14}$$

where $\dot{m}$ and w_{CH_4} are local values. Note that is not a simple average of the radial profiles of composition, which yields a result sometimes remarkably different. The averaging above reflects the physical process that actually takes place in the empty spaces between catalyst segments, i.e. mixing of the 'layers' of fluid that exit the channel at different radial position. Similarly, the temperature measurements cannot retain any distinction among radial positions inside the channel and represent the values resulting from an adiabatic mixing of the layers inside the channels:

$$\dot{m} H(T(z_k), \bar{\mathbf{w}}) = \int_A \dot{m} H(T, \mathbf{w}) \tag{15}$$

Unfortunately, the enthalpy is a nonlinear function of T because of $C_p(T)$, so the evaluation of such adiabatic mixing temperature requires the solution of a nonlinear equation at each point z_k. On the other hand, since the reactions is modeled through the single conversion of CH_4 to CO_2 and H_2O, and the channels are assumed adiabatic, the temperature at any point can be given by Eq. (13), where the conversion $\xi(z)$ is easily evaluated from $\bar{w}_{CH_4}$. Such considerations about the proper averaging of T and w_{CH_4} help to understand the actual mechanism of the process. Consequences are discussed below, where the model of

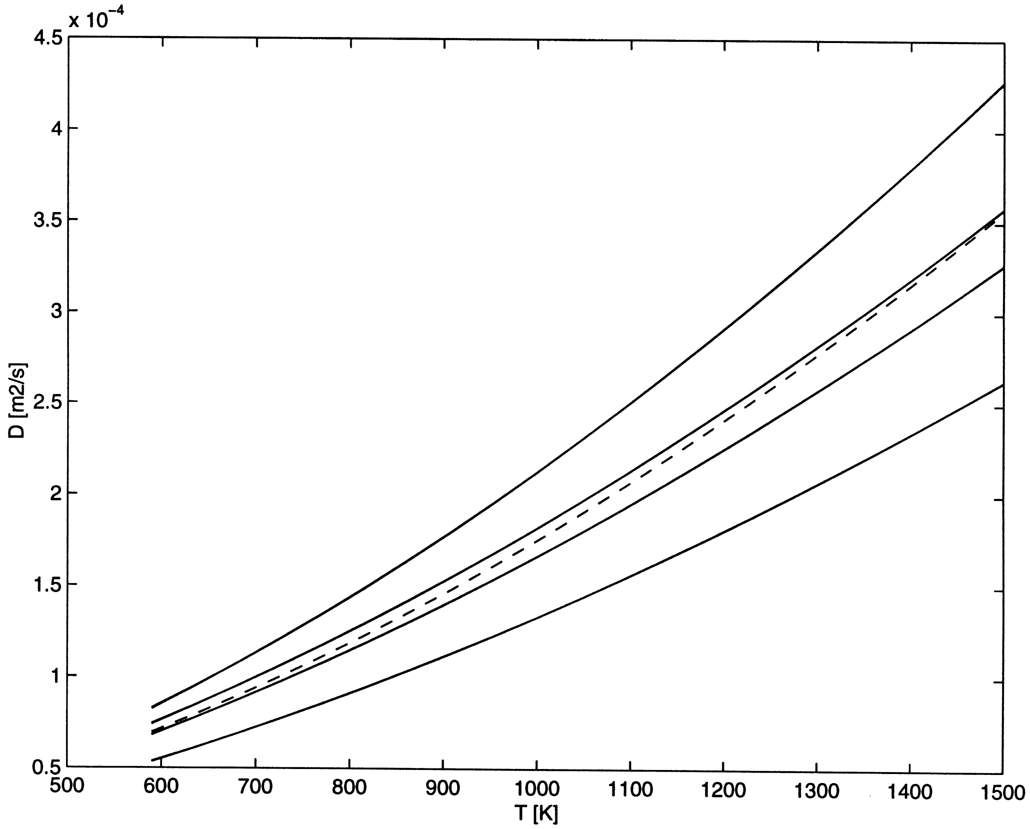

Fig. 3. Binary diffusion coefficients of H_2O, CH_4, O_2, and CO_2 (from the top) in N_2. The dashed curve is the correlation of Fuller et al. [37] for CH_4–N_2.

continuous channel is compared to a model where the monolith is truly segmented, with intermediate mixing.

Among the three experiments reported in [31], the one at higher equivalence ratio is the most significant. The ignition and the diffusive regime are clearly distinguishable, while other tests barely ignite the mixture. At the conditions of the experiment the regime is definitely laminar. The Reynolds number varies between 77 and 157, at the inlet and outlet, respectively. According to established correlation the length required to fully develop the velocity profile in a pipe with our diameter is between 0.012 and 0.016 m. Since the monolith wafers are 0.02 m long, it can be concluded that even a non-reacting laminar flow takes most of the length of the wafer to develop an asymptotic velocity profile. On the other hand, modeling the four segments as a single channel clearly disregard the alternating disruption and development of the velocity profile in the channels.

First, we attempted to model the data in Table 1 using the parameter values reported in the literature [26] for Eq. (11). Such a combination of parameters and kinetic equation results in an abrupt ignition, not shown by the experiments, that makes the convergence extremely difficult. Again, concerns about the consistency of the parameter values and units arise. The results shown in Fig. 1 are obtained reducing the preexponential factor by orders of magnitude, as reported in the caption. Both temperature and conversion profiles are reported, although the first is a linear transformation of the second. Because of that, only $C(z)$ profiles will be shown in the following. From Fig. 1, it can be concluded that Eq. (11) with literature values of the parameters yields a rate of methane conversion which is too high compared with the experimental results. It

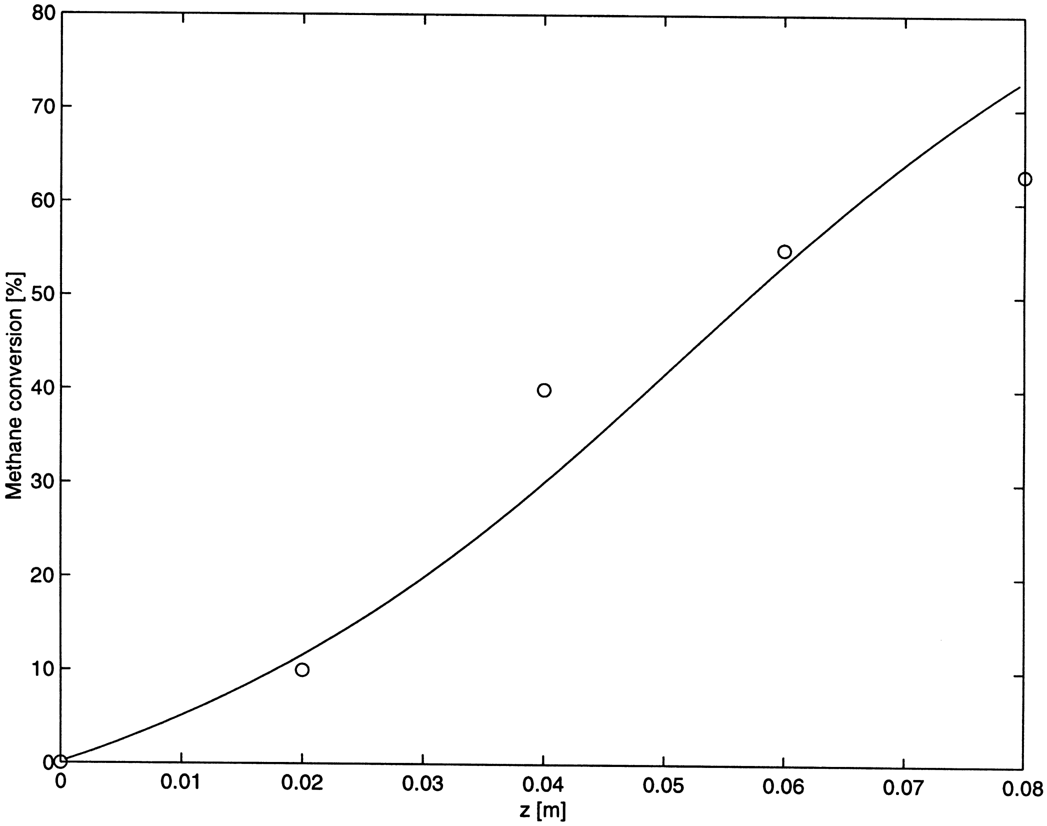

Fig. 4. Conversion profile from a continuous channel model. Best-fit of A and E_a in a global reaction. $A = 8.66 \times 10^5\,\mathrm{cm}^{5/2}\,\mathrm{s}^{-1}\,\mathrm{g}^{-1/2}$, $E_a = 60.72\,\mathrm{kJ/mol}$. Data from [31] at $\phi = 0.39$.

is not clear, though, whether such a behavior can be explained by a poor description of the chemistry or by the values of the physical parameters, particularly diffusion coefficients. We started observing that the conversion–length curve after ignition closely resembles the case of a 1D model with instantaneous reaction at the wall. For sake of comparison, Fig. 2 shows the results of our model with increasing reaction rate. To simplify, temperature dependence of k has been inhibited and k used as a parameter to vary the reaction rate, looking for the threshold of diffusion control. It is interesting to note that even with a high reaction rate our simulation shows a rather small diffusion limitation. With the values of $\mathcal{D}_{i,\mathrm{N}_2}(T, P)$ that we used, reaction is almost always controlling. The conversion increases very rapidly, because of rather high diffusion coefficients, increasing even more with temperature. Fig. 3 shows the variation of the binary diffusion coefficients with T at 1 bar, from 850 to 1500 K. The value of 1.2 for the Schmidt number ($\mu/\rho\mathcal{D}$) adopted in [10] results in a diffusion coefficient up to five times smaller than predicted here at high temperature. The effect of a reduction of the binary diffusion coefficients is investigated in the same Fig. 2, where the actual $\mathcal{D}_{i,\mathrm{N}_2}(T, P)$ functions have been divided by 2. A completely different behavior is observed with a significant reduction of the overall conversion. Note that the relevance of diffusion coefficients once in the mass transfer limited regime is tantamount to that of reaction rate constants. Accordingly, the dotted line in Fig. 1 has been obtained with the literature parameters for A and E_a, but $\mathcal{D}_{i,\mathrm{N}_2}(T)$ have been reduced by an order of magnitude. Such a test is not purely parametric, since a similar reduction results in values of diffusion coefficients close to the value at ambient conditions, $\mathcal{D}_{i,\mathrm{N}_2}$ (298 K, 1 bar), i.e. those usually

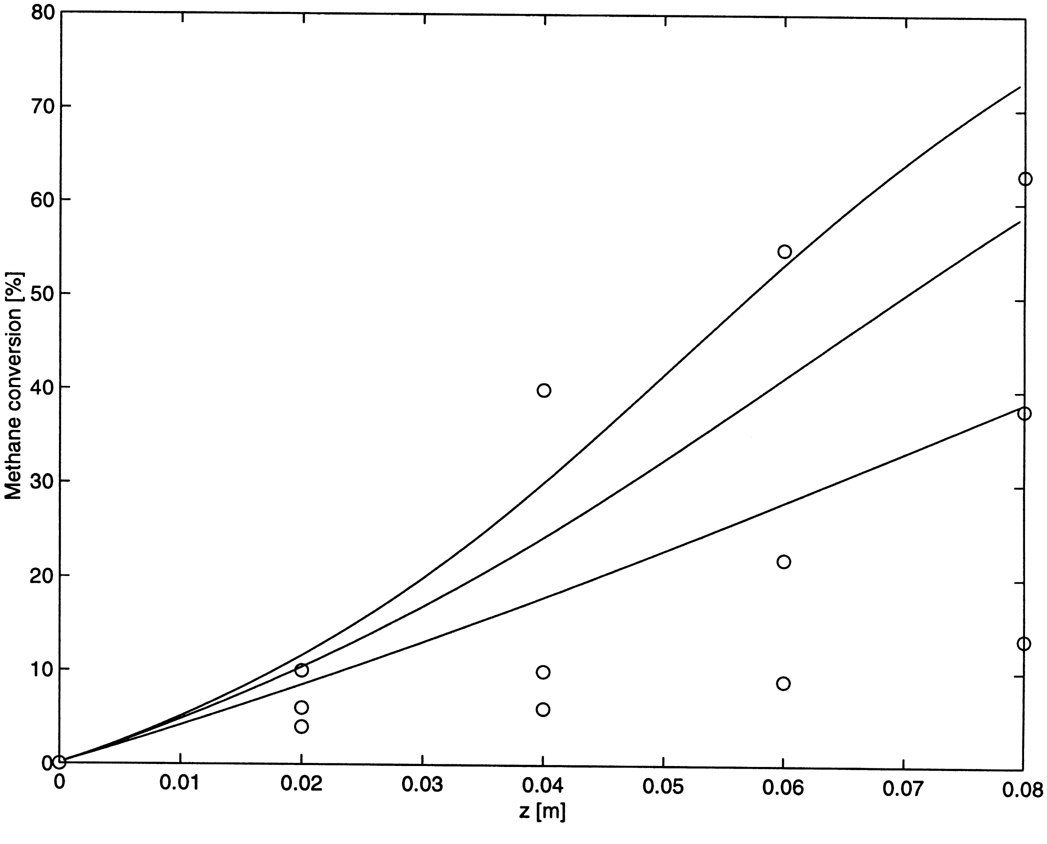

Fig. 5. Conversion profile from a continuous channel model. Simulation of three experimental data set ($\phi = 0.18, 0.30, 0.39$) with kinetic parameters obtained from the case of $\phi = 0.39$ ($A = 8.66 \times 10^5\,\mathrm{cm}^{5/2}\,\mathrm{s}^{-1}\,\mathrm{g}^{-1/2}$, $E_\mathrm{a} = 60.72\,\mathrm{kJ/mol}$). Data from [31].

reported in the literature [24]. In our model the values of $\mathcal{D}_{i,\mathrm{m}}$ has been approximated to the value of the binary coefficients, assuming that species other than N_2 are highly diluted. Taking into account also the composition dependency of $\mathcal{D}_{i,\mathrm{m}}$ can easily lead to adjustments comparable with the test of Fig. 2. We can conclude that the role of diffusion coefficients is extremely relevant. Constant values can easily result in meaningless predictions. The functions $\mathcal{D}_{i,\mathrm{N}_2}(T, P)$ that we introduced provide more realistic values but result in a weaker diffusion limitation than usually observed.

In the description of the model above, we concluded that kinetic equations and parameters in global reaction rate expressions could have other values with different catalysts. Accordingly, we set up an optimization procedure, based on standard routines [36]. The whole model is solved many times for changing values of A and E_a, searching the set that minimizes the errors in the prediction of the experimental values. This is a rather important point: a kinetics investigation of reactive systems like catalytic combustion can hardly uncouple the chemical process from the physical ones. The mechanism can be identified only through a model that correctly accounts for the transport processes.

The best-fit of the experimental data at higher CH_4 concentration in the feed ($\phi = 0.39$) is shown in Fig. 4. The estimated parameter values are $A = 8.66 \times 10^5\,\mathrm{cm}^{5/2}\,\mathrm{s}^{-1}\,\mathrm{g}^{-1/2}$, $E_\mathrm{a} = 60.72\,\mathrm{kJ/mol}$. The activation energy turns out to be much smaller than reported, although Trimm and Lam [13] already observed a distinct change above 813 K (i.e. below the inlet temperature of this experiment), where he estimated an activation energy of 86 kJ/mol. The value of the preexponential factor shows six orders of magnitude difference with literature value. That is certainly

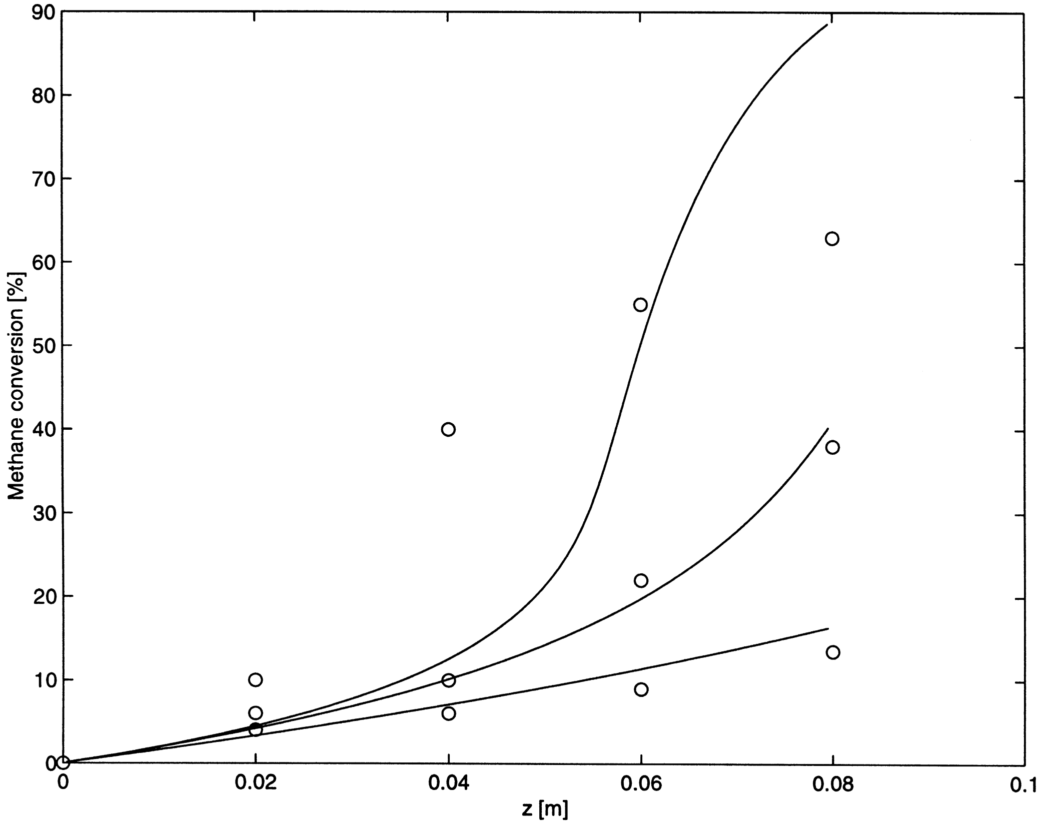

Fig. 6. Conversion profile from a continuous channel model. Fitting the kinetic parameters to experimental values of three data set ($\phi = 0.18, 0.30, 0.39$). $A = 1.05 \times 10^{10}\,\mathrm{cm}^{5/2}\,\mathrm{s}^{-1}\,\mathrm{g}^{-1/2}$, $E_\mathrm{a} = 101\,\mathrm{kJ/mol}$. Data from [31].

due to the lower value of the activation energy, but it can also be caused by different composition variables in Eq. (11). The agreement observed in Fig. 4 is rather unsatisfactory. Tracking the search for the optimal parameters, it can be observed that higher values of A and E_a are sought, but then the reaction gets too fast, once ignited, whereas the diffusion is not limiting the conversion enough. The parameters estimated are a compromise, still quite poor. It can be a clear evidence that more detailed chemistry is required, possibly only an additional reaction, in the gas phase. More likely, results call for an even more precise description of the mass transfer process. Fig. 5 shows the comparison of all the experimental data for different inlet composition and the prediction obtained with the parameters estimated above. It can be easily concluded that the low value of the activation energy does not account for the ignition delay shown by the data.

Searching for the kinetic parameters that give the best agreement with all the data available at the same time, we obtained the results shown in Fig. 6. The best-fit is given by $A = 1.05 \times 10^{10}\,\mathrm{cm}^{5/2}\,\mathrm{s}^{-1}\,\mathrm{g}^{-1/2}$, $E_a = 101\,\mathrm{kJ/mol}$. The measurements where a clear light-off is not evidenced ($\phi = 0.18$ and 0.30) are the majority (eight data out of a total of 12). These data call for a higher activation energy in order to account for a more difficult ignition with the temperature. On the other hand, the data at higher fuel ratio are poorly explained by the parameter values above. The experimental data at $\phi = 0.39$ clearly show a diffusive limitation toward the reactor outlet (higher temperature) not reproduced by our simulation. Unsuccessful attempts were made to modify the error function weighting differently both the first measurement, closer to the inlet, and the different data set. It is confirmed that a simple attempt to fit the experimental data [31] acting

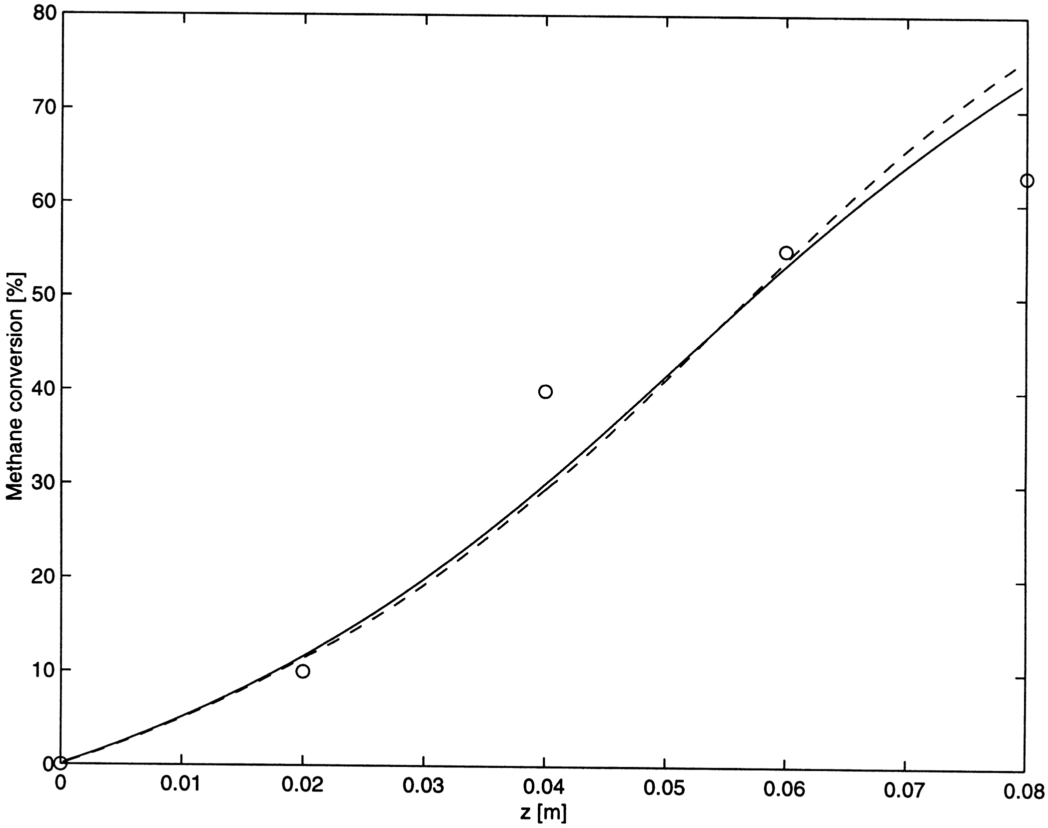

Fig. 7. Conversion profile: (solid line) continuous channel model; (dashed line) wafers with intermediate mixing. Data from [31] at $\phi = 0.39$.

purely on the chemical kinetics, with a single step, is not satisfactory.

An additional analysis has been performed in order to estimate the significance of the assumption of a continuous channel for the sequence of wafers. The empty spaces in between the catalytic wafers destroy the flow structure inside the channel. An adiabatic mixing process takes place in the gaps so that the boundary conditions at the inlet of subsequent wafer are completely different from the outlet of the previous one. A simulation has been performed assuming that the inlet of each segment has a uniform composition, velocity, and temperature profiles. Values are determined by Eqs. (14) and (15). The adiabatic mixing temperature of Eq. (15) determines the density. Results are shown in Fig. 7 for the richer feed ($\phi = 0.39$). A small difference is observed with respect to the continuous channel scheme. Larger discrepancies should be observed if the diffusion process were slower, because of its sensitivity to radial composition profiles. The same analysis for the leaner mixtures ($\phi = 0.18$ and 0.30) yields even less significant differences, since the conversion is lower and the radial concentration profiles poorly affected by intermediate mixing between wafers. Note that these results could be a consequence of an overestimation of the diffusion coefficients, already observed.

The same data discussed above have been modeled also by the authors of the measurements [31] with the reactive boundary layer code CRESLAF [33] in conjunction with detailed mechanism for both the gas and the surface reactions [11,34] from GRI and [35], respectively. Rather good results are reported although the temperature of the catalyst surface has been adapted to fit the data. The choice is rather unusual, since an adiabatic reactor cannot have a single wall temperature. Nevertheless, the code [33] needs the surface temperature for the evaluation of kinetic constants. That results in uncoupling of surface and gas phase temperatures, which is rather unlikely.

5. Conclusions

The catalytic combustion is a process extremely stimulating for the many issues still open to investigation. The identification of a proper kinetic mechanism to overtake the empiricism of global reactions is tightly coupled to many physical processes, heavily influenced by the reaction because of the large heat release. At the same time, the experimental investigation is difficult because of the sensitivity of the process and the difficulty of the measurements, whose scale is often much larger than the actual process taking place at or near the surface. The development of adequate kinetic equations from experimental data goes through a detailed modeling of the physics of the process, the relevance of which is often underestimated. Diffusion coefficients have been shown to be frequently more critical than kinetic parameters. The need to account for varying geometry and flow arrangements found in practical applications suggests to use well established fluid dynamics codes. Their use as part of the kinetic investigation has been shown here to be promising.

References

[1] L.D. Pfefferle, W.C. Pfefferle, Catal. Rev.-Sci. Eng. 29 (1987) 219.
[2] L.C. Young, B.A. Finlayson, AIChE J. 22 (1976) 331, 343.
[3] S.T. Kolackowski, Catal. Today 47 (1999) 209.
[4] L.D. Pfefferle, Catal. Today 26 (1995) 255.
[5] G. Groppi, A. Belloli, E. Tronconi, P. Forzatti, Chem. Eng. Sci. 50 (1995) 2705.
[6] S.H. Oh, J.C. Cavendish, Ind. Eng. Chem. Prod. Res. Dev. 21 (1982) 29.
[7] T. Ahn, W.V. Pinczewski, D.L. Trimm, Chem. Eng. Sci. 41 (1986) 55.
[8] K. Zygourakis, Chem. Eng. Sci. 44 (1989) 2075.
[9] R.E. Hayes, S.T. Kolackowski, W.J. Thomas, J. Titiloye, Ind. Eng. Chem. Res. 35 (1996) 406.
[10] X. Song, W.R. Williams, L.D. Schmidt, R. Aris, Comb. Flame 84 (1991) 292.
[11] M.E. Coltrin, R.J. Kee, F.M. Rupley, Surface Chemkin (Ver. 4.0): a Fortran package for analyzing heterogeneous chemical kinetics at a solid-surface–gas-phase interface, Sandia National Laboratories Report SAND90-8003C, 1994.
[12] O. Deutschman, F. Behrendt, J. Warnatz, Catal. Today 46 (1998) 155.
[13] D.L. Trimm, C.W. Lam, Chem. Eng. Sci. 35 (1980) 1405.
[14] R.E. Hayes, S.T. Kolackowski, Chem. Eng. Sci. 49 (1994) 3587.
[15] F. Moallemi, G. Batley, V. Dupont, T.J. Foster, M. Porkashanian, A. Williams, Catal. Today 47 (1999) 235.
[16] Y. Tsujikawa, S. Fujii, H. Sadamori, S. Ito, S. Katsura, Catal. Today 26 (1995) 267.
[17] R. Jahn, D. Snita, M. Kubicek, M. Marek, Catal. Today 38 (1997) 39.
[18] J.A.M. Kuipers, W.P.M. van Swaaij, Rev. Chem. Eng. 13 (1997) 1.
[19] CFX 4.2: Solver Manual, AEA Technology, 1998.
[20] R.B. Bird, W.E. Stewart, E.N. Lightfoot, Transport Phenomena, Wiley, New York, 1960.

[21] S.V. Patankar, Numerical Heat Transfer and Fluid Flow, Hemisphere, Washington, DC, 1980.
[22] P. Stopford, AEA Technology, personal communication, 1998.
[23] R.J. Kee, G. Dixon-Lewis, J. Warnatz, M.E. Coltrin, J.A. Miller, A Fortran computer code package for the evaluation of gas-phase multicomponent transport properties, Sandia National Laboratories Report SAND89-8009B, 1994.
[24] R.C. Reid, J.M. Prausnitz, B.E. Poling, The Properties of Gases and Liquids, 4th Edition, McGraw-Hill, New York, 1987.
[25] R.E. Hayes, S.T. Kolackowski, Catal. Today 47 (1999) 295.
[26] P. Markatou, L.D. Pfefferle, M.D. Smooke, Comb. Flame 93 (1993) 185.
[27] R. Mezaki, C.C. Watson, Ind. Eng. Chem. Proc. Des. Dev. 5 (1966) 62.
[28] M.D. Rumminger, R.D. Hamlin, R.W. Dibble, Catal. Today 47 (1999) 253.
[29] J.A. Dumesic, D.F. Rudd, L.M. Aparicio, J.E. Rokoske, A.A. Treviño, The Microkinetics of Heterogeneous Catalysis, ACS, Washington, DC, 1993.
[30] D. Papadias, M.F.M. Zwinkels, L. Edsberg, P. Björnbom, Catal. Today 47 (1999) 315.
[31] T.C. Bond, R.A. Noguchi, C.P. Chou, R.K. Mongia, J.Y. Chen, R.W. Dibble, in: Proceedings of the 26th Symposium on Combustion, The Combustion Institute, 1996, 1771 pp.
[32] W.C. Reynolds, STANJAN-III, Version 3.8C, Stanford University, Stanford, CA, 1988.
[33] M.E. Coltrin, H.K. Moffat, R.J. Kee, F.M. Rupley, CRESLAF(Ver. 4.0): a Fortran program for modeling laminar chemically reacting, boundary-layer flow in cylindrical or planar channels, Sandia National Laboratories Report SAND93-0478, 1993.
[34] R.J. Kee, F.M. Rupley, J.A. Miller, Chemkin-II: a Fortran chemical kinetics package for the analysis of gas phase chemical kinetics, Sandia National Laboratories Report SAND89-8009, 1989.
[35] O. Deutschman, F. Behrendt, J. Warnatz, Catal. Today 21 (1994) 461.
[36] B.S. Garbow, K.E. Hillstrom, J.J. More, Minpack Project, Argonne National Laboratory, France, 1980.
[37] E.N. Fuller, P.D. Schettler, J.C. Giddings, Ind. Eng. Chem. 58 (1966) 19.